this observation sits more comfortably with the earlier mechanism than with recent proposals.

Conclusions

The present work confirms that large amounts of useful information may be obtained through application of modern NMR techniques to ^{3}H. Different methods have applicability under different circumstances.

Double quantum filtering (or more general multiple quantum filtering) is quite useful for isolating ^{3}H coupled ^{3}H multiplets. Since isotope shifts and coupling constants are very similar in magnitude (at this field strength) complex "multiplets" may arise from either. Filtering allows for identification of true coupled multiplets with the possibility for selection based on the number of spins involved. The drawback is that excitation of different multiplets may not be uniform (due to differences in coupling constant), and hence intensities in filtered spectra may not accurately reflect the concentration of any particular species in solution.

Polarization transfer methods (DEPT or INEPT) also offer some opportunities for introducing selectivity into experiments. In this case the selection method depends upon T–H couplings rather than T–T. As such it will be useful for distinguishing among molecules with different numbers of protons equivalently coupled to tritons. As with multiple quantum filtering methods, the limitation arises from the frequent lack of equivalence in coupling constants and the resulting non-uniformity of excitation.

J-resolved experiments are quite powerful in analysis of mixtures of isotopic species. Since *both* 1° and 2° isotope shifts are larger than line widths, and all T–T couplings appear only in the ω_1 dimension, many different closely related isotopomers can be distinguished. The experiment does not require selection based on coupling constant, hence it can be quite quantitative, and problems are likely to occur only in the case of strong couplings among the tritons. The small number of experiments required in ω_1 makes this a faster experiment than 2D correlated spectroscopy. Ambiguities which arise from combined isotope shifts from several neighbors may be resolved through multiple quantum filtering or RELAY types of experiments when concentrations of such species are high enough.

Correlated experiments, including both T–T COSY and T–H correlation, perform as expected, but they require relatively long acquisition times and high sample activities. Often spectra are simple enough that chemical shifts and multiplicities can establish the labeling pattern. However, when the presence of neighboring tritons must be established the T–T COSY will be useful, and similarly the T–H correlated experiment can help establish the presence of specific T–H pairs. Other correlated experiments (RELAY, multiple quantum 2D, etc.) will probably not be regularly used due to low sensitivity and to the fact that extended coupled T networks do not usually result from common labeling schemes.

It is important to note that the distribution of labeled products from even a simple "hydrogenation" reaction is complex. When a complete understanding of the isotope distribution in products is required the multiple pulse NMR methods will be very important. It is clear that simple notions about reaction mechanisms may be approximately followed, but there are likely to be many side products (at small to moderate concentrations) that will also have to be considered. "Hidden" reactions at allylic positions could prejudice stereochemical yields in many routine hydrogenation reactions.

Acknowledgment. P.G.W. and H.M. are supported by the Biotechnology Resources Program, Division of Research Resources, U.S. National Institutes of Health under Grant P41 RR01237-06, and by the U.S. Department of Energy under Contract DE-AC03-76SF00098. D.E.W. also thanks the Health Effects Research Division, OHER, of the U.S. Department of Energy for continuing support.

Registry No. PhCHTCHTCH$_3$, 117067-85-3; PhCH$_2$CHTCH$_3$, 117067-86-4; PhCT$_2$CHTCT$_3$, 117067-87-5; *cis*-β-methylstyrene, 766-90-5; *trans*-β-methylstyrene, 873-66-5; tritium, 10028-17-8; *n*-propylbenzene, 117067-88-6.

Electron Spin Resonance and Electron Spin Echo Spectroscopic Studies of Catalytic Dimerization of Ethylene on Palladium-Exchanged Na–X and Ca–X Zeolites. Proposed Reaction Mechanism for Ethylene Dimerization

Ashim K. Ghosh and Larry Kevan*

Contribution from the Department of Chemistry, University of Houston, Houston, Texas 77004.

Received February 22, 1988

Abstract: Both NaPd–X and CaPd–X zeolites are shown to dimerize ethylene selectively to *n*-butenes after an induction period, which is decreased with an increase of palladium content and is less for CaPd–X than for NaPd–X due to location of more Pd species at sites accessible to ethylene. A shorter induction period is also seen at higher reaction temperature due to migration of Pd species toward sites accessible to ethylene. Paramagnetic Pd$^+$ species C ($g_\parallel = 2.53$) and D ($g_\parallel = 2.33$–2.34), both with $g_\perp$ values of 2.10, are observed to form prior to ethylene dimerization and have been assigned to Pd$^+$–C$_2$H$_4$ and Pd$^+$–(C$_2$H$_4$)$_2$, respectively. These species are considered to be active intermediates for the reaction. When ethylene is dimerized to butene, paramagnetic species, assigned to Pd$^+$ coordinated to butenes, are observed. Ethylene dimerization on the Pd-exchanged zeolites is suggested to occur via coordination of two ethylene molecules to a Pd$^+$ paramagnetic species. The initial 1-butene product is isomerized to an equilibrium composition of *n*-butenes with *trans*-2-butene predominant. All catalysts are found to deactivate during ethylene dimerization probably due to reduction of Pd species to atomic Pd.

Palladium-exchanged zeolites are used as catalysts for hydrocracking,[1] hydrogenation,[2,3] and dimerization of small olefins.[4–9] However, little work has been done on the nature of the active palladium species or on its site and immediate environment in the

0002-7863/88/1510-8044$01.50/0

zeolite.

Several papers have treated ethylene dimerization on Pd-exchanged zeolites.[4-9] It is generally accepted that palladium species directly participate in the formation of catalytically active sites. In a previous study,[10] we have shown that paramagnetic species, giving ESR signals at $g_{\parallel} = 2.53$ and $g_{\parallel} = 2.33-2.34$, both with $g_{\perp}$ at 2.10, assigned to Pd^+ coordinated to ethylene, are detected prior to butene formation. Consequently, monovalent palladium cations in Pd-exchanged X zeolites are considered to be catalytically active sites for ethylene dimerization. In all cases, the catalyst was found to deactivate during the dimerization reaction. The ESR signals for Pd^+ complexes significantly decrease or disappear at a longer reaction time, and the catalyst deactivation was interpreted as due to reduction of Pd^+ ions to atomic Pd.

The more abundant cocations influence the location and coordination of active cations in zeolite[11] and hence the catalytic activity.[10] In NaPd-X zeolite, palladium cations occupy sites SI or SI′, which are relatively inaccessible to ethylene, while in CaPd-X zeolites palladium cations occupy sites SII′ or SII, which are relatively accessible to ethylene. As a result, the reaction occurs after a longer induction period in NaPd-X zeolites due to migration of palladium species toward accessible locations.[10]

Recently, using electron spin resonance (ESR) and X-ray photoelectron spectroscopic methods, we have been able to characterize various Pd^+ complexes in NaPd-X and CaPd-X zeolites and to propose their locations in the zeolite lattice.[12] The weak hyperfine interactions of a paramagnetic species with the surrounding nuclei in the lattice provide useful structural information. This cannot normally be measured by conventional ESR methods due to resolution limitations. However, in recent years the powerful technique of electron spin echo modulation (ESEM) spectroscopy has been developed to measure these weak hyperfine interactions.[13-17]

The present work describes the results of ethylene dimerization on Pd-exchanged Na-X and Ca-X zeolites by using a static reactor. With ESR spectroscopy, the generation and migration of paramagnetic species are monitored before and during the ethylene reaction. In order to obtain information on the immediate environment of the active catalytic site, ESEM spectra are recorded for zeolites with adsorbed C_2D_4. The catalyst deactivation mechanism is discussed, and a reaction mechanism for ethylene dimerization on Pd-exchanged zeolites is proposed.

Experimental Section

Linde Na-X zeolite was obtained from Alpha Chemicals. Ca-X zeolite was prepared from Na-X by ion exchange with 0.1 M $CaCl_2$ solution at 80 °C for 1 week. Palladium was introduced into the zeolite as $Pd(NH_3)_4^{2+}$ cation by ion exchange with various amounts of 0.01 M palladium tetraamine chloride (Alpha) solution at room temperature for 24 h. Commercial atomic absorption was used to determine the palladium content. Most experiments were done with samples of $CaPd_{9.6}$-X and $NaPd_{12.5}$-X zeolites where the subscript refers to the number of palladium ions per unit cell. Some experiments were done with Na-X, Ca-X, $CaPd_{1.7}$-X, and $NaPd_{1.6}$-X zeolites. Ethylene and deuteriated ethylene were obtained from the Linde Division of the Union Carbide Corp. and MSD Isotopes, respectively.

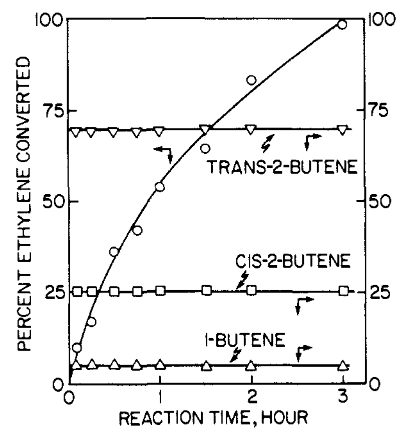

Figure 1. Ethylene dimerization on O_2-pretreated $CaPd_{9.6}$-X zeolite. Reaction conditions: catalyst 0.05 g, $P^0_{C_2H_4}$ = 400 Torr, reaction temperature 50 °C.

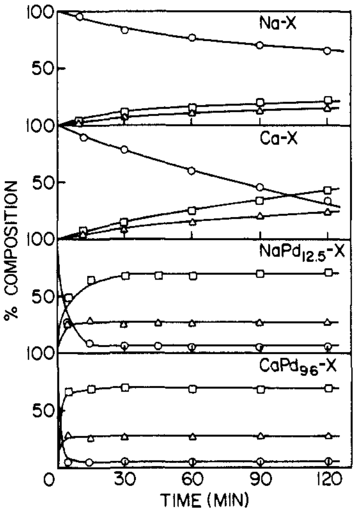

Figure 2. Isomerization of 1-butene on O_2-pretreated zeolites. Reaction conditions: catalyst 0.05 g, $P^0_{1\text{-}C_4H_8}$ = 400 Torr, reaction temperature 50 °C. Key: ○, 1-butene; ▲, *cis*-2-butene; □, *trans*-2-butene.

Experiments were carried out with a fixed-bed-type reactor made of glass with a closed, static reactor system of total internal volume of about 58 cm^3. A zeolite sample of 0.05 g was placed on a sintered-glass disk inside the reactor. The zeolite was heated in oxygen flow (30 cm^3/min) while the temperature was slowly increased to 500 °C at which heating was continued for 16 h.

Ethylene dimerization was studied on the O_2-pretreated zeolite samples by introducing a measured quantity of ethylene (0.65 mmol) into the reactor containing pretreated zeolite at a specific reaction temperature. The reaction products were analyzed at different reaction times by withdrawing aliquots for analysis by an on-line gas chromatograph (Varian Model 3300 equipped with an electronic integrator with a thermal conductivity detector using a 6-ft. column (i.d. 0.085 in.) packed with 0.19 wt % picric acid on 80/100-mesh Graphic GC support at 35 °C). The initial rate of ethylene dimerization was calculated from the initial butene formation. Isomerization of 1-butene was also studied on O_2-pretreated Na-X, Ca-X, $NaPd_{12.5}$-X, and $CaPd_{9.6}$-X at a reaction temperature of 50 °C by using a static reactor.

The generation and migration of paramagnetic palladium species in the system was examined by ESR. The reactor was connected to a small quartz tube (3-mm o.d.) so that the ESR spectrum could be recorded without exposure of the sample to air. Both before and after various amounts of ethylene reaction, the sample was quenched to room temperature and transferred in situ to the ESR tube. ESR spectra were immediately recorded at 77 K with a Varian E-4 spectrometer. Electron spin echo spectra were recorded at 4.2 K with a home-built spectrometer.[16,17] Deuteriated ethylene was used for ESEM measurements in order to detect and analyze deuterium modulation.

---

(1) Bolton, A. P. In *Zeolite Chemistry and Catalysis*; Rabo, J. A., Ed.; American Chemical Society: Washington, DC, 1976; Chapter 13.
(2) U.S. Patent 3544565, 1972.
(3) Minachev, Kh. M.; Garanin, V. I.; Kharlamov, V. V.; Isakova, T. A. *Kinet. Katal.* **1972**, *13*, 1101.
(4) U.S. Patent 3738977, 1973.
(5) Lapidus, A. L.; Mal'tsev, V. V.; Garanin, V. I.; Minachev, Kh. M.; Eidus, Ya. T. *Izv. Akad. Nauk SSSR, Ser. Khim.* **1975**, 2819.
(6) Lapidus, A. L.; Mal'tsev, V. V.; Shpiro, E. S.; Antoshin, G. V.; Garanin, V. I. Minachev, Kh. M. *Izv. Akad. Nauk SSSR, Ser. Khim.* **1976**, 2454.
(7) Lapidus, A. L.; Mal'tsev, V. V. *Acta Phys. Chem.* **1978**, *24*, 195.
(8) Lapidus, A. L.; Minachev, Kh. M. *Neftekhimiya* **1978**, *18*, 212.
(9) Michalik, J.; Lee, H.; Kevan, L. *J. Phys. Chem.* **1985**, *89*, 4282.
(10) Ghosh, A. K.; Kevan, L. *J. Phys. Chem.* **1988**, *92*, 4439.
(11) Narayana, M.; Kevan, L. *Langmuir* **1985**, *1*, 553.
(12) Narayana, M.; Michalik, J.; Contarini, S.; Kevan, L. *J. Phys. Chem.* **1985**, *89*, 3895.
(13) Mims, W. B. *Phys. Rev. B: Solid State* **1972**, *B5*, 2409.
(14) Salikhov, K. M.; Semenov, A. G.; Tsvetkov, Yu. D. *Electron Spin Echoes and Their Applications*; Science: Novosibirsk, 1976.
(15) Kevan, L. In *Time Domain Electron Spin Resonance*; Kevan, L., Schwartz, R. N., Eds.; Wiley-Interscience: New York, 1979; Chapter 8.
(16) Ichikawa, T.; Kevan, L.; Narayana, P. A. *J. Phys. Chem.* **1979**, *83*, 3378.
(17) Narayana, P. A.; Kevan, L. *Magn. Reson. Rev.* **1983**, *1*, 234.

Table I. Ethylene Dimerization on O_2-Pretreated Palladium-Exchanged Na–X and Ca–X Zeolites

catalyst	reaction time, °C	induction period, min	initial rate, mmol g^{-1} h^{-1}
$NaPd_{1.6}$–X	85	90	1.4
$NaPd_{12.5}$–X	25	[a]	
	50	60	5.6
	85	0	12.5
$CaPd_{1.7}$–X	25	30	2.0
$CaPd_{9.6}$–X	25	15	2.9
	50	0	9.3
	85	0	13.0

[a] Only a trace amount of butenes was detected after a 4-h reaction period.

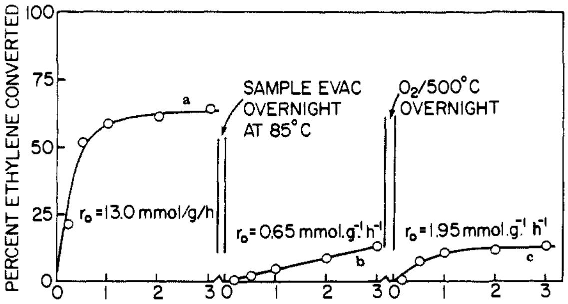

Figure 3. Ethylene dimerization on O_2-pretreated $NaPd_{12.5}$–X zeolite. Reaction conditions: catalyst 0.05 g, $P^0_{C_2H_4}$ = 400 Torr, reaction temperature 85 °C. Key: (a) fresh sample, (b) after reaction sample was evacuated at 85 °C for 16 h, (c) after reactions in (a) and (b) (sample was heated in O_2 flow at 500 °C for 16 h).

Results

A. Ethylene Dimerization. A typical catalytic run of ethylene dimerization is shown in Figure 1. It shows that ethylene is dimerized to an equilibrium composition of *n*-butenes. It is reported[9,18,19] that ethylene is first dimerized to 1-butene, which is subsequently isomerized to *cis*- and *trans*-2-butenes. We have also studied isomerization of 1-butene on O_2-pretreated Na–X, $NaPd_{12.5}$–X, Ca–X, and $CaPd_{9.6}$–X zeolites at a reaction temperature of 50 °C (see Figure 2). These catalysts were found to be active for isomerization of 1-butene to *cis*- and *trans*-2-butenes. The initial rate of isomerization increases in the order Na–X < Ca–X ≪ $NaPd_{12.5}$–X < $CaPd_{9.6}$–X. In Na–X and Ca–X zeolites, the butene isomers did not reach the equilibrium ratio in 2 h. However, the *n*-butenes reach the equilibrium ratio in about 5 and 30 min in $CaPd_{9.6}$–X and $NaPd_{12.5}$–X zeolites, respectively.

The results of ethylene dimerization on various Pd-exchanged X zeolites are summarized in Table I. The initial rate of dimerization increases with the palladium content of the zeolite due to an increase in the number of active palladium sites. This reaction occurs on Pd-exchanged zeolites after an induction period, which decreases with an increase of palladium content in the zeolite, reaction temperature and CaPd–X zeolite versus NaPd–X zeolite. Under the same experimental conditions, higher catalytic activity, defined by the initial rate of dimerization, was observed for CaPd–X zeolites in comparison to NaPd–X zeolites.

In all cases, the rate of conversion of ethylene to butenes decreases at a longer reaction time. This decrease is more pronounced at a higher reaction temperature. For example, in O_2-pretreated $NaPd_{12.5}$–X the conversion of ethylene to butene increases almost linearly, after an induction period, to nearly 100% conversion at 50 °C (not illustrated), but at 85 °C the sample becomes almost inactive for ethylene dimerization in about 1 h of reaction (Figure 3a). This once used catalyst was evacuated overnight at 85 °C to desorb any products and unreacted ethylene, and then the catalyst was again tested for ethylene dimerization (Figure 3b). This evacuation procedure did not enhance the dimerization reaction efficiency to any significant extent. The rate of ethylene dimerization was found to be 0.65 mmol g^{-1} h^{-1}, which is 20-fold less in comparison to that observed with a fresh $NaPd_{12.5}$–X sample. Pretreated zeolite (orange or light brown) became grey or light black when the catalyst was almost inactive. This may be due to reduction of palladium cations to atomic Pd or coke deposition on the catalyst. The twice-used catalyst was heated in O_2 flow at 500 °C overnight and then was found to be slightly more catalytically active than a once-used catalyst but significantly less catalytically active in comparison to a fresh sample.

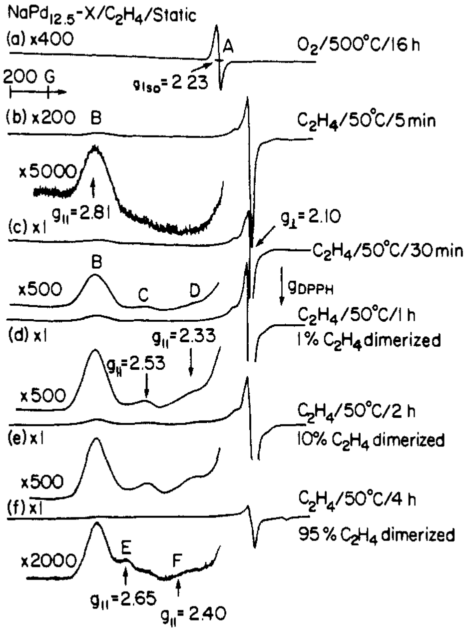

Figure 4. ESR spectra of $NaPd_{12.5}$–X at 77 K: (a) after pretreatment under O_2 flow at 500 °C, and (b–f) at different reaction times in the presence of ethylene in a static reactor at 50 °C.

B. Electron Spin Resonance Studies. The generation of paramagnetic species in palladium-exchanged Na–X and Ca–X zeolites is sensitive to the concentration of Pd^{2+} cations and to the pretreatment conditions of the catalysts. In previous work,[20,21] an isotropic ESR signal at g_{iso} = 2.23 was assigned to Pd^{3+} species, and anisotropic ESR signals with $g_{\parallel}$ = 3.0–2.3 and $g_{\perp}$ = 2.10 were assigned to Pd^+ species. The ESR signal at g_{iso} = 2.23, designated as species A, was generated in both NaPd–X and CaPd–X zeolites after pretreating the zeolites in O_2 flow at a temperature of 500 °C.

Signal A, attributed to Pd^{3+} species, disappeared on exposure of the zeolite to ethylene. Concomitantly, signals B ($g_{\parallel}$ = 2.81), C ($g_{\parallel}$ = 2.53), and D ($g_{\parallel}$ = 2.34) with the same $g_{\perp}$ value at 2.10 are observed to form prior to detection of ethylene dimerization products in the gas phase (Figure 4). The appearance of the ESR signals and the formation of the products are dependent on the adsorption (reaction) temperature. For example, at 25 °C in case of the $NaPd_{12.5}$–X sample species B appeared on ethylene admission, but no other species except for a very weak signal C appeared during a 4-h reaction period. Only about 0.1% ethylene dimerized on $NaPd_{12.5}$–X at 25 °C during a 4-h period. At higher temperatures of 50, 65, and 85 °C, in addition to species B, strong signals C and D appeared with simultaneous ethylene dimerization. It has been previously concluded that species B, attributed to Pd^+ ions, is situated in a location inaccessible to ethylene in the zeolite structure and cannot coordinate ethylene.[10] However, the Pd^+ cations may subsequently migrate to a location accessible to ethylene where ethylene may coordinate with them to result in species C and D. Subsequently, ethylene is dimerized to butenes. These results suggest that Pd^+ ions are involved in the dimerization

---

(18) Bonneviot, L.; Olivier, D.; Che, M. *J. Mol. Catal.* **1983**, *21*, 415.
(19) Yashima, T.; Ushida, M.; Ebisawa, M.; Hara, N. *J. Catal.* **1975**, *36*, 320.
(20) Michalik, J.; Heming, M.; Kevan, L. *J. Phys. Chem.* **1986**, *90*, 2132.
(21) Michalik, J.; Narayana, M.; Kevan, L. *J. Phys. Chem.* **1985**, *89*, 4553.

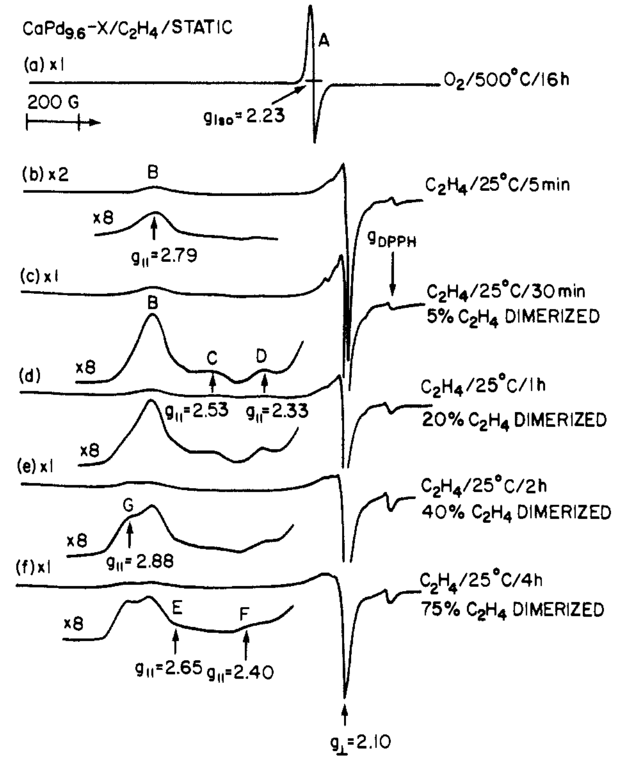

Figure 5. ESR spectra of $CaPd_{9.6}$–X at 77 K: (a) after pretreatment under O_2 flow at 500 °C, and (b–f) at different reaction times in the presence of ethylene in a static reactor at 25 °C.

reaction. Species E ($g_\parallel$ = 2.65) and F ($g_\parallel$ = 2.40) with the same $g_\perp$ value at 2.10 were observed at higher ethylene conversion. These species are attributed to Pd^+ ions at different sites complexed with butenes.[10]

As observed in the case of $NaPd_{12.5}$–X, signal A in O_2-pretreated $CaPd_{9.6}$–X zeolite disappears on exposure to ethylene, and subsequently species B–D appear. It is important to note that the species B–D appear in $CaPd_{9.6}$–X zeolite at a lower reaction temperature than in $NaPd_{12.5}$–X zeolite (Figure 5). At 25 °C in $CaPd_{9.6}$–X species C and D are observed together with ethylene dimerization, while this does not occur in $NaPd_{12.5}$–X at 25 °C. As in $NaPd_{12.5}$–X zeolite, at a higher conversion of ethylene species E and F are observed in $CdPd_{9.6}$–X together with an additional species G ($g_\parallel$ = 2.88, $g_\perp$ = 2.10).

Figure 6 shows ESR spectra of a $NaPd_{12.5}$–X sample at various conditions of ethylene dimerization and catalyst deactivation. As shown earlier, the paramagnetic species, B–D, observed during ethylene dimerization, decrease significantly or disappear as the catalyst deactivates. The ESR spectrum of the once-used catalyst was not changed significantly after evacuation of the sample. As mentioned earlier, this evacuation did not improve the catalytic activity. The ESR spectrum recorded after heating the twice-used catalyst in O_2 flow at 500 °C showed a broad peak at $g_\parallel$ = 2.70 (line width ~800 G) and an isotropic signal at g_{iso} = 2.00. The former peak seems to be due to Pd^+ ions coordinated to unknown organic molecules, which could be formed during heating of the used catalyst. The isotropic signal at g_{iso} = 2.00 may be assigned to organic free radicals.

C. ESEM Studies. Pretreated samples of NaPd–X and CaPd–X show too small an ESEM signal to study echo modulation. As mentioned earlier, species A in $NaPd_{12.5}$–X, attributed to Pd^{3+} ions, disappears on exposure of the pretreated zeolite to ethylene, and then species B appears initially at room temperature. No spin echo is observed for samples showing species B. However, at higher temperatures, when species C and D are observed, strong echo signals and deuterium modulation are observed at a magnetic field set at $g_\perp$(B–D) = 2.10. If all species B–D have a contribution to the modulation, the ESEM analysis would be ambiguous. But field-sweep experiments show that at magnetic fields at $g_\parallel$(C) = 2.53 and $g_\parallel$(D = 2.34 echo signals are observed but that at $g_\parallel$ = 2.81 (signal B) the echo disappears (Figure 7). These results suggest that the observed modulation for the palladium–ethylene complex is mostly due to signals C and D. As shown in Figures 8 and 9, simulation of these data indicates that species C is due to Pd^+ ions interacting with one C_2D_4 molecule with a Pd–D distance of 0.43 nm and that species D is due to Pd^+ ions interacting with two C_2D_4 molecules with four deuteriums at a Pd–D distance of 0.42 nm and the other four deuteriums at a Pd–D distance of 0.49 nm.

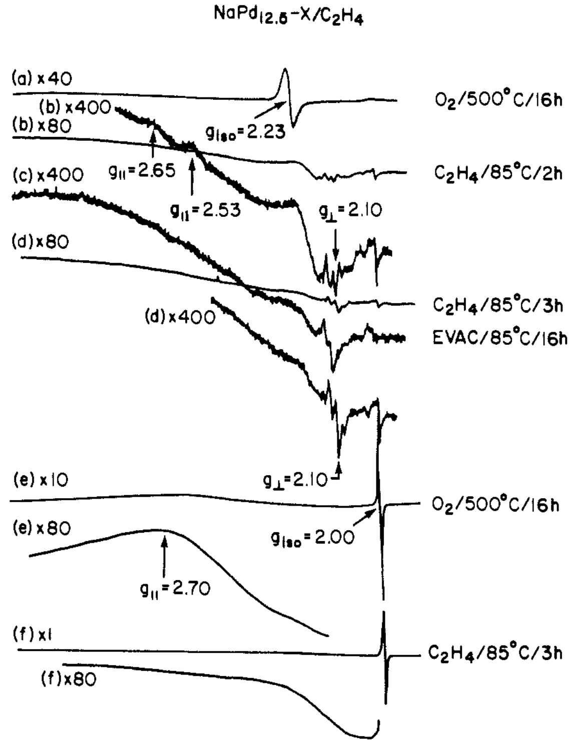

Figure 6. ESR spectra at $NaPd_{12.5}$–X at 77 K: (a) O_2-pretreated at 500 °C, (b) ethylene dimerization reaction on the O_2-pretreated sample, (c) once-used catalyst sample was evacuated at 85 °C for 16 h, (d) ethylene dimerization on the evacuated sample, (e) twice-used catalyst was heated in O_2 flow at 500 °C for 16 h, and (f) ethylene dimerization reaction on catalyst heated in O_2. Reaction conditions for (b), (d), and (f) are the same as described in Figure 3.

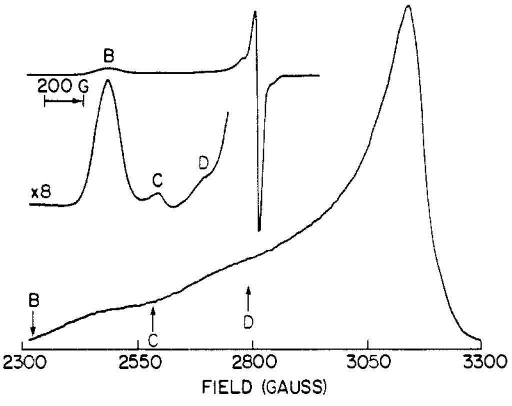

Figure 7. Field-swept ESE spectrum at 4 K of $NaPd_{12.5}$–X with adsorbed C_2D_4. The ESR spectrum of the sample at 77 K is shown in the inset.

As in $NaPd_{12.5}$–X zeolite, ESR signals B–D are also observed in $CaPd_{9.6}$–X zeolite during ethylene dimerization. Strong echo signals and deuterium modulation are observed at a magnetic field set at $g_\perp$(B–D) = 2.10. In a field-sweep ESE experiment, it was not possible to distinguish between the contributions of species C and D to the deuterium modulation. The Pd^+–ethylene complex may be converted to reaction products faster in the case of CaPd–X zeolite than in NaPd–X zeolite. However, the ESEM analysis of the spectra recorded at magnetic fields set at $g_\parallel$(C) = 2.53 (Figure 10) and at $g_\parallel$(D) = 2.33 (Figure 11) indicates that

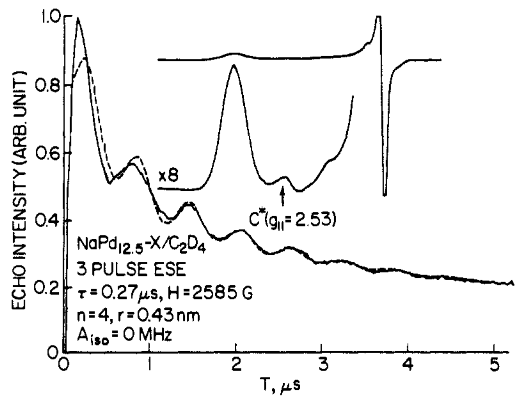

Figure 8. Experimental (—) and simulated (---) three-pulse ESEM spectra at a 4 K of $NaPd_{12.5}$–X with adsorbed C_2D_4 at 50 °C for 2 h recorded at the magnetic field set at $g_\parallel = 2.53$ indicated by an asterisk on the inset of the ESR spectrum at 77 K.

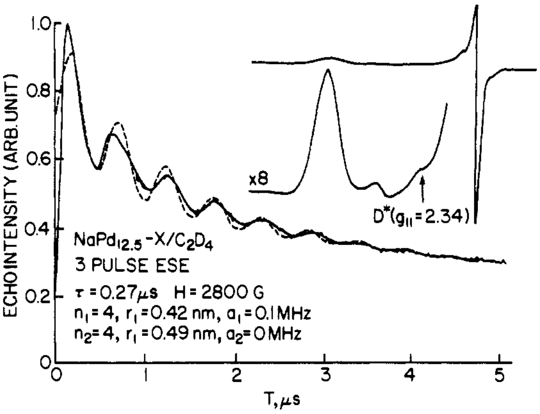

Figure 9. Experimental (—) and simulated (---) three-pulse ESEM spectra at 4 K of $NaPd_{12.5}$–X with adsorbed C_2D_4 at 50 °C for 2 h recorded at the magnetic field set at $g_\parallel = 2.34$ indicated by an asterisk on the inset of the ESR spectrum at 77 K.

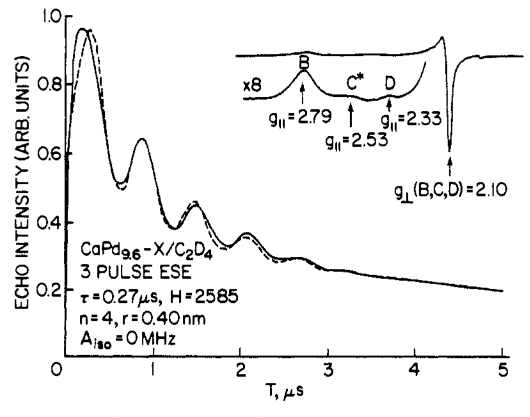

Figure 10. Experimental (—) and simulated (---) three-pulse ESEM spectra at 4 K of $CaPd_{9.6}$–X with adsorbed C_2D_4 at 25 °C for 30 min recorded at the magnetic field set at $g_\parallel = 2.53$ indicated by an asterisk in the inset of the ESR spectrum at 77 K.

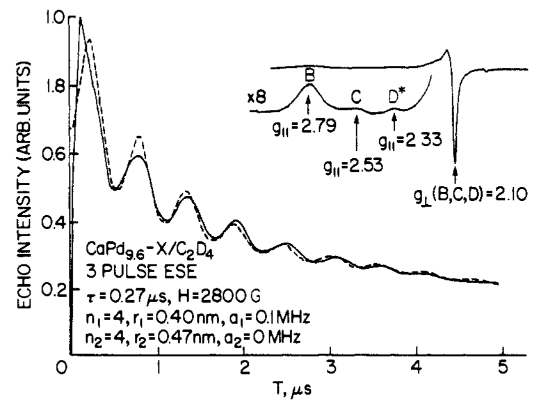

Figure 11. Experimental (—) and simulated (---) three-pulse ESEM spectra at 4 K of $CaPd_{9.6}$–X with adsorbed C_2D_4 at 25 °C for 30 min recorded at a magnetic field set at $g_\parallel = 2.33$ indicated by an asterisk in the inset of the ESR spectrum at 77 K.

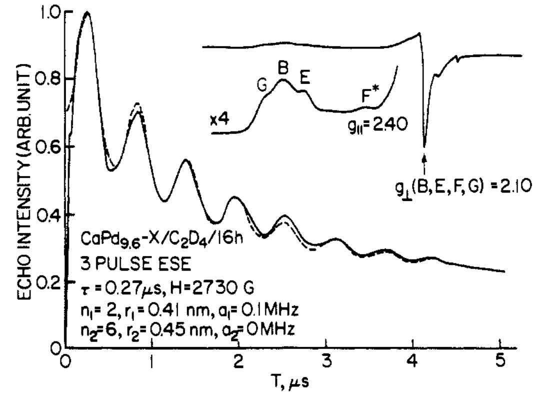

Figure 12. Experimental (—) and simulated (---) three-pulse ESEM spectra at 4 K of $CaPd_{9.6}$–X with adsorbed C_2D_4 at 25 °C for 16 h recorded at the magnetic field set at $g_\parallel = 2.40$ indicated by an asterisk in the inset of the ESR spectrum at 77 K.

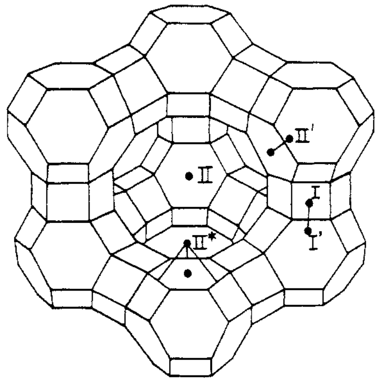

Figure 13. Cation sites and their designations in X zeolite.

species C is due to Pd^+ ions interacting with one C_2D_4 molecule with a Pd–D distance of 0.40 nm and that species D is due to Pd^+ ions interacting with two C_2D_4 molecules with four deuteriums at a Pd–D distance of 0.40 nm and the other four deuteriums at a Pd–D distance of 0.47 nm.

Species E–G, attributed to Pd^+ ions at different zeolite sites coordinated to butenes,[10] in addition to species B, are observed in the ESR spectrum of $CaPd_{9.6}$–X on which C_2D_4 was adsorbed at 25 °C for 16 h (Figure 12). Field-sweep ESE experiments show that the echo disappears at magnetic fields set at $g_\parallel = 2.79$ (signal B) and $g_\parallel = 2.88$ (signal G). A very weak spin echo was observed at a magnetic field set at $g_\parallel = 2.65$ (signal E) and was too weak to study echo modulation. Deuterium echo modulation was recorded at a magnetic field set at $g_\parallel = 2.40$ (signal F). The simulated spectrum is consistent with our catalytic and ESR results that species F may be attributed to Pd^+ complexed with one butene molecule with two deuteriums at a Pd–D distance of 0.41 nm and another six deuteriums at a Pd–D distance of 0.45 nm.

Discussion

Zeolite X is composed of alternating AlO_2 and SiO_2 tetrahedra with a Si/Al ratio of 1.25. These units are linked to form truncated octahedra called sodalite cages or β-cages, which are tetrahedrally bonded through a double six-ring unit called a hexagonal prism to form larger supercages called α-cages. The free apertures to the α-cage and β-cage are 0.74 and 0.22 nm, respectively. Due to the excess negative charge present on the AlO_2 units, compensating cations are present to balance the charge in the zeolite framework. Figure 13 shows various cation sites identified by X-ray crystallography.[22] Site SI is the center of the hexagonal prism, SI′ is a site displaced from SI into the β-cage, SII is the center of the hexagonal window between the β-cage and the α-cage, and SII′ and SII* correspond to displacement from site SII into the β-cage and into the α-cage, respectively, along an axis perpendicular to the hexagonal window.

A. Ethylene Dimerization. In a previous work,[10] we have shown that Na–X and Ca–X zeolites are catalytically inactive for ethylene dimerization. Pd-exchanged Na–X and Ca–X zeolites are shown to be catalytically active for ethylene dimerization. These results confirm that Pd species directly participate in the formation of catalytically active sites. In this work, ethylene is dimerized to *n*-butenes selectively, and the butenes reach an equilibrium ratio during the reaction time.

It has been reported that ethylene is initially dimerized to 1-butene, which is subsequently isomerized to an equilibrium composition of *n*-butenes with predominant *trans*-2-butene over various transition-metal cation-exchanged zeolites.[9,18,19] In the present work, isomerization of 1-butene, formed during ethylene dimerization, occurs very rapidly and reaches an equilibrium ratio at the reaction temperature. The parent Na–X zeolite is shown in Figure 2 to be active for 1-butene isomerization even at a low reaction temperature of 50 °C. The exchange of Na^+ by Ca^{2+} ions increases the zeolite activity for isomerization. It is important to note that when the Pd^{2+} ions are exchanged for Na^+ or Ca^{2+} ions, the zeolite activity increased quite significantly for 1-butene isomerization. This agrees with previous work, which showed faster 1-butene isomerization in $CaPd_2$–X in comparison to Ca–X zeolite.[9]

In this work, all the catalysts were found to deactivate at longer reaction times. This deactivation is most pronounced at higher reaction temperature. The deactivation may be ascribed to one or more of the following reasons: (i) instability of active palladium cations, (ii) pore blocking of the zeolite catalyst, and (iii) deposition of coke on the catalyst during the reaction. In the present work, various paramagnetic Pd^+ species are observed to form prior to dimerization of ethylene. The paramagnetic species were found to decrease at longer reaction times with a simultaneous decrease of catalytic activity. The catalyst turns brown to grey or light black after the reaction. These results imply that the active palladium cations are unstable under the reaction conditions and are likely converted to atomic Pd, which are catalytically inactive for ethylene dimerization.[6,7] In a XPS study, Lapidus et al.[6] have shown that ethylene reduces cationic palladium (Pd^{2+} and Pd^+) in NaCaPd–Y to Pd^0 during ethylene dimerization on the catalyst at 50 °C. The color of the catalyst changed from brown to black, as also found by treatment with H_2.

The dimerization reaction must occur in the zeolite supercage considering the size of ethylene and butenes, which cannot enter or leave the β-cage or the hexagonal prism. The evacuation of a once-used zeolite sample at 85 °C for 16 h should remove any physisorbed or weakly bonded ethylene and butenes. However, evacuation of a once-used sample did not improve the catalytic activity of the sample. This does not rule out the possibility of zeolite pore blockage by more strongly interacting olefins if present. However, the catalyst deactivation increases at higher temperature, which argues against deactivation due to pore blocking by olefins. If coke formation were the main deactivation mechanism, oxygen exposure at elevated temperature should burn off coke depositions and increase the catalyst activity. However, this was not found. It seems most likely that the reduction of Pd species to Pd^0 is the main source of deactivation. One might expect oxygen treatment at elevated temperature to oxidize zero-valent palladium species, but after such oxygen exposure, the used catalyst did not regain its original ESR spectrum.

B. Palladium–Ethylene Complex Formation and Induction Period. The complex $Pd(NH_3)_4{}^{2+}$ ions, exchanged into Na–X and Ca–X zeolites, occupy site SV at the center of the α-cage due to size considerations. In the course of thermal pretreatment of the zeolite under gas flow, some rearrangement of the cations in the zeolite cages can occur. The Pd complex also decomposes thermally above 300 °C to generate Pd^{2+} cations, which migrate into the β-cage or hexagonal prism. In NaPd–X zeolite, Pd^{2+} species occupy preferentially site SI′ in the β-cage. Previous ESEM studies[20] in this laboratory have demonstrated that Pd^{3+} ions are formed by oxidation of Pd^{2+} in NaPd–X and further migrate to a more protected site SI in the center of the hexagonal prism. The Pd^{3+} ion exposed to D_2O and ND_3 gives interaction distances of Pd^{2+}–D(D_2O) and Pd^{3+}–D(ND_3), which are consistent with Pd^{3+} ions at SI. In contrast, Pd^{2+} ions in CaPd–X occupy site SII′ due to the high affinity of Ca^{2+} ions for site SI′ in the β-cage. Pd^{3+} ions from oxidation of Pd^{2+} may further migrate to the more accessible site SII between the α- and β-cages.

The ethylene molecules (kinetic diameter 0.39 nm) are too bulky to enter the β-cage or in the hexagonal prism of the zeolite. So, the formation of a palladium–ethylene complex requires the migration of Pd cations toward the α-cage. On adsorption of ethylene in NaPd–X zeolite, species B appears initially, but no dimerization reaction occurs. Simultaneously, species A, attributed to Pd^{3+} ions, disappears, indicating their reduction to Pd^{2+} ions, a part of which is then further reduced to Pd^+ ions. This reduction mechanism is not clearly understood but is suggested[23,24] to occur via an electron transfer from ethylene molecule to an electron acceptor site of the zeolite framework, which in turn reduces the palladium cation since the ethylene molecules cannot enter the β-cage or hexagonal prism, which the palladium cations initially occupy. Species B may be due to either Pd^+ ions or Pd^+ ions weakly coordinated to ethylene at a long distance. The ESR signal intensity of species B was not decreased by evacuation of the sample overnight, suggesting that species B may be due to Pd^+ ions. Our ESE results are not conclusive because no spin echo was observed when only species B was observed during ethylene interaction. It should be emphasized that Pd^+ ions generated during high-temperature evacuation of O_2-pretreated samples give different ESR parameters ($g_\parallel = 3.01$, $g_\perp = 2.10$).[10,20,21]

Species C and D appear simultaneously prior to butene formation and are assigned to Pd^+–ethylene complexes as active intermediate species for ethylene dimerization.[10] The present ESE results confirm that species C and D are due to Pd^+–C_2H_4 and Pd^+–$(C_2H_4)_2$ complexes, respectively. When the ethylene is converted to butenes, paramagnetic species E and F (and an additional species G in the case of CaPd–X) are observed. It is not possible to conclude from our ESE results alone, but we speculate that species G may be due to Pd^+ ions and E may be due to Pd^+ ions weakly coordinated to butene at a long distance. Species F is assigned to Pd^+ ions coordinated to one molecule of butene, as supported by the present ESE results.

Ethylene dimerization is found to occur on both NaPd–X and CaPd–X zeolites after an induction period. This induction period is dependent on the type of cocation (Na^+ or Ca^{2+}), the amount of Pd content in the zeolite, and the reaction temperature. This has been previously explained as due to different locations of the active palladium cations.[10] As mentioned earlier, Pd^{3+} and Pd^{2+} ions in pretreated zeolite occupy inaccessible sites in the β-cage or hexagonal prism to which ethylene cannot approach closely. In order to form a Pd–ethylene complex, Pd cations must migrate toward the α-cage. In CaPd–X zeolite, the migration of Pd cations occurs more rapidly than those in NaPd–X zeolite since Pd cations in CaPd–X occupy sites closer to the α-cage (SII′ or SII) in comparison to the sites in NaPd–X (site SI′ or SI). Also at higher cation exchange, after preferential occupation of site SI′ (NaPd–X) or SII′ (CaPd–X) Pd cations are likely to occupy relatively accessible sites. The migration of exchangeable cations also is expected to occur more rapidly at higher temperature. This explains the decrease of the induction period at higher temperature.

C. Proposed Reaction Mechanism. The present ESR results show that species A, attributed to Pd^{3+} ions, disappears on ex-

---

[22] Smith, J. V. In *Zeolite Chemistry and Catalysis*; Rabo, J. A., Ed.; American Chemical Society: Washington, DC, 1976; Chapter 1.

[23] Bergeret, G.; Tri, T. M.; Gallezot, P. *J. Phys. Chem.* **1983**, *87*, 1160.

[24] Romanikov, V. N.; Ione, G. G.; Pedersen, L. A. *J. Catal.* **1980**, *66*, 121.

posure of the zeolite sample to ethylene and that species B, attributed to Pd^+ ions, appears immediately, indicating that reduction of Pd^{3+} and Pd^{2+} to Pd^+ cations by ethylene occurs rapidly. The Pd^+ ions so formed migrate toward the α-cage to interact with ethylene. Our ESR and ESE results suggest that initially one molecule of ethylene interacts with a Pd^+ ion, giving a π-complex identified as species C, followed by the addition of another ethylene molecule to the same Pd^+ ion, giving an intermediate identified as species D. Bonneviot et al.[18] have suggested that two molecules of ethylene are π-bonded to Ni^+ in Ni–X zeolite for dimerization. The intermediate complex D is postulated to undergo a geometric isomerization to bring the two ethylene molecules into a favorable position for the reaction to form 1-butene, which is then isomerized to *cis*- and *trans*-2-butene. Since the zeolite is shown to be highly active for 1-butene isomerization, an equilibrium composition of *n*-butenes is observed even in the early stages of product formation. The proposed reaction mechanism is shown below.

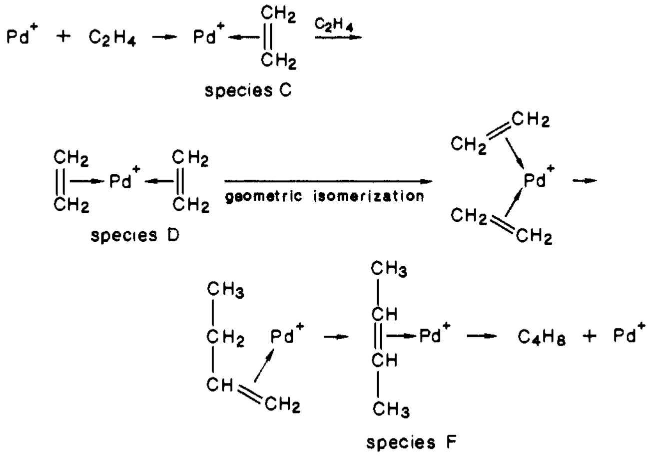

Conclusions

Ethylene dimerization occurs on both NaPd–X and CaPd–X zeolites after an induction period. The catalytic activity increases with an increase of Pd content in the zeolite due to an increase of active Pd sites. The reaction induction period is found to decrease with increase of Pd content or reaction temperature. It is also less for CaPd–X zeolite in comparison to NaPd–X zeolite due to the different Pd species locations. In CaPd–X zeolite, Pd^{2+} ions occupy site SII′ due to the strong affinity of Ca^{2+} ions for site SI′. But in NaPd–X zeolite Pd^{2+} ions occupy site SI′. A part of the Pd^{2+} ions, during O_2-pretreatment, are oxidized to Pd^{3+} ions, which migrate to site SII, a more accessible site to ethylene, in CaPd–X zeolite. However, in NaPd–X zeolite the Pd^{3+} ions migrate to site SI in the hexagonal prism of the zeolite structure. In the presence of ethylene, the Pd cations are reduced to Pd^+ ions and migrate toward the α-cage for coordination with ethylene molecules. The formation of paramagnetic species B–D is observed prior to ethylene dimerization, and it is concluded that monovalent Pd cations are the active species for the dimerization reaction. The present ESE results confirm that species C and D are due to $Pd^+–C_2H_4$ and $Pd^+–(C_2H_4)_2$ complexes, respectively. Paramagnetic $Pd^+–C_4H_8$ complexes are also detected when most of the ethylene is converted to butenes. In a proposed reaction mechanism ethylene dimerization on Pd-exchanged Na–X and Ca–X zeolites is suggested to occur via the addition of two ethylene molecules to the same Pd^+ cation. In ethylene dimerization, 1-butene is initially formed and is subsequently isomerized to *cis*- and *trans*-2-butene. These catalysts are deactivated at longer reaction times and higher temperatures most likely due to reduction of active Pd^+ ions to atomic palladium.

Acknowledgment. This research was supported by the National Science Foundation (Grant CHM-8514108) and the Texas Advanced Technology Research Program.

Registry No. Pd, 7440-05-3; ethylene, 74-85-1; 1-butene, 106-98-9.

Nonplanarity of the Methylcyclobutyl Cation

Martin Saunders* and Norbert Krause†

Contribution from the Department of Chemistry, Yale University, New Haven, Connecticut 06511-8118. *Received March 21, 1988*

Abstract: α,β,α′-Trideuteriated methylcyclobutyl cation was prepared and studied in the NMR to look for isotopic perturbation of the inversion of a possibly nonplanar structure, without interference from the known rapid process that interchanges the nonequivalent methylene groups. Observation of a splitting in the ^1H NMR spectrum of the deuteriated ion with intensity ratio of 2:1 unambiguously demonstrates that the cation is nonplanar. A temperature-dependent downfield shift of the proton peaks in the deuteriated ion was also observed and may indicate a rapid equilibrium with a minor species.

Phenomena involving the ready ionization of cyclobutyl and cyclopropylcarbinyl derivatives to form cationic intermediates have been studied for many years. We have wanted to learn the structures and energies of all significant intermediates and transition states involved. Recently, the stable $C_4H_7^+$ ion formed from either cyclobutyl or cyclopropylcarbinyl precursors[1] has been shown by NMR deuterium isotopic perturbation[2] and high-level quantum mechanical calculations[3] to be a rapidly equilibrating set of three degenerate nonclassical bicyclobutonium ions and three degenerate cyclopropylcarbinyl cations, quite different in geometry, yet very close in energy and interconverting rapidly over a very flat energy surface.[3] Introduction of a methyl group to produce an analogous ion, which is formally tertiary, might be expected to alter the situation to favor classical structure and behavior. However, the experimental results indicate distinctly nonclassical behavior for methylcyclobutyl cation.

Ionization of methylcyclobutyl chloride or alcohol in $SbF_5–SO_2ClF$ solution to yield a $C_5H_9^+$ cation (**1**) was reported in 1970.[4]

[†] Postdoctoral Fellow at Yale University, 1987–1988.

(1) Olah, G. A.; Prakash, G. K. S.; Sommer, J. *Superacids*; Wiley: New York, 1985; pp 143–146.

(2) Saunders, M. "The Effect of Isotopic Perturbation on NMR Spectra. A New Method for Distinguishing Rapidly Equilibrating Molecules from Symmetric Molecules". *Stereodynamics of Molecular Systems*; Sarma, R. H., Ed.; Pergamon: Elmsford, NY, 1979; pp 171–184.

(3) Saunders, M.; Laidig, K. E.; Wiberg, K. B.; Schleyer, P. v. R. *J. Am. Chem. Soc.*, in press.

0002-7863/88/1510-8050$01.50/0